Asian Journal of Chemistry Vol. 22, No. 4 (2010), 2615-2624

Ultrasonic Assisted Synthesis and Characterization of Yttrium Aluminum Garnet (YAG) Powders

MIAO SHUI*, YIFAN ZHENG†, YUE SONG, QINGCHUN WANG and YUANLONG REN
State Key Laboratory Base of Novel Functional Materials and Preparation Science, Faculty of Materials Science and Chemical Engineering, Ningbo University, Zhejiang-315211, P.R. China
Fax: (86)(574)87600734; Tel: (86)(574)87600147; E-mail: shuimiao@nbu.edu.cn

Yttrium aluminum garnet (YAG) precursors were synthesized by co-precipitation method assisted by high power intermittent ultrasonic with high initial reactant concentration (2.0 mol/L). Yttrium aluminum garnet began to crystallize when calcinated for 2 h at relatively low temperature (800 ºC) without the appearance of such intermediate phase as YAP and YAM. Rietveld refinement software GASA was used to refine the structural parameters and size information. TG/DTA, FT-IR methods were used to characterize the composition and thermal stability of the precursors. SEM/EDS measurements revealed the coating structure of two components in precursors and the morphology of YAG being flakes with 200-300 nm long and 60-70 nm wide agglomerated by 60-70 nm YAG grain in the case of YAG precursor calcinated for 2 h at 1100 ºC.

Key Words: High power intermittent ultrasonic, Co-precipitation, Yttrium aluminum garnet, Rietveld refinement.

INTRODUCTION

Yttrium aluminum garnet ($Y_3Al_5O_{12}$, YAG) has been paid much attention because of its better optical and high-temperature mechanical properties[1]. Yttrium aluminum garnet is cubic in structure and does not exhibit any birefringence effects at the grain boundaries, showing a variety of good optical properties. Doping with other rare earth ions, such as Nd^{3+}, Ce^{3+} *etc.* into YAG makes it an ideal material for phosphors and high power solid-state lasers. Recently, the quality of the Nd:YAG ceramics has been improved greatly and highly efficient laser oscillation is obtained[2]. Moreover, as a high temperature structural ceramics, YAG shows excellent chemical stability and creep resistance[3]. Recently it is reported that the creep rate of polycrystalline YAG (3 μm grain size) stressed at 75.5 MPa at 1400 ºC is only one third of that of the polycrystalline Al_2O_3 tested under equivalent conditions. Besides that, YAG is an ideal liquid phase sintering promoter for the preparation of silicon

†Research Center for Analysis and Measurement, Zhejiang University of Technology, Zhejiang-310014, China.

carbide ceramics with high performance at low-temperatures. Owing to such a wide and diverse application potential for YAG-based materials, new methods of synthesis of pure and highly dispersed YAG powder with specific morphology is desirable.

Yttrium aluminum garnet (YAG) powder was traditionally produced by a solid state reaction[4] between the component oxides which requires repeated mechanical mixing, prolonged grinding time and extensive heat treatment at temperatures as high as 1700 ºC to eliminate YAM and YAP intermediate phases. Other preparation methods include sol-gel[5], hydrothermal[6], combustion synthesis[7], spray pyrolysis and precipitation[8]. Sel-gel method needs expensive alkoxide precursors and produce indispensible large amount of waste water to be treated. Combustion synthesis and hydrothermal method require complicated and specialized facilities usually with lower yield. Precipitation method is widely used for simple synthesis process, lower cost, commonly available apparatus, being suitable for commercial manufacturing. However, severe agglomeration often occurs during drying, causing poor sinterability of the resultant YAG powders. To obtain evenly distributed powder with specific morphology, the species of precipitant, precipitation conditions should be carefully chosen and low concentration reactants are usually applied resulting in large amount of wastewater.

We know that ultrasonic has complicated physical and chemical effects in liquid-phase system. Physical effect includes mass transfer and heat transfer while chemical effect derives from acoustic cavitations. Air bubbles excited by ultrasonic form, grow, contract, re-grow and re-contract in liquid. Ultimately, they collapse at high speed and release huge energy, generate high-speed (110 mS^{-1}) micro jet flow. According to the "hot spot" theory, extreme temperature (5000 K), high pressure (1000 atm) and high cooling or heating rate (> 10^{10} K/S) occur within the bubbles during cavitational collapse. Under these extreme conditions, the preceding reactions like hydrolysis and oxidation-reduction reaction followed by nucleation and growth can be accelerated by more times. Therefore, large quantities of nuclei are formed simultaneously. The abrasion and collision between the nano-particles carried by jet flow or turbulent flow are supposed to lower the chance of nuclei growth and coagulation.

According to the theory of crystal nucleation and crystal growth, critical radius of nuclei is supposed[9] to be $r = \frac{2V}{3k_B T \ln(S)}$. To obtain evenly distributed (mono-disperse), small-sized particles, a short nucleation period where large quantities of nuclei nucleate all of a sudden and short period of self-sharpening growth are favourable conditions. Nearly mono-disperse size distribution can be obtained by either starting or stopping the reaction (nucleation and growth) quickly or by supplying reactant source to keep the super-saturation of the solute to a steady level. It is observed that the intermittent ultrasonic pulse applied in the solution is in favour of the formation of even-sized particles.

The present studies report an easy ultra-high power ultrasonic assisted route for the synthesis of evenly dispersed, yttrium aluminum garnet (YAG) precursors,

which begins to crystallize calcinated at 800 ºC for 2 h without the appearance of intermediate phase like YAM and YAP, *etc.* The morphology, micro-structure, spectral character of YAG powders are also characterized.

EXPERIMENTAL

The yttrium and aluminum sources used for YAG synthesis are yttrium oxide (99.99 %) and analytically pure $Al(NO_3)_3 \cdot 9H_2O$, respectively. Analytical reagent ammonium hydrogen carbonate (AHC) is used as precipitants. The stock solution of mother salts is made by dissolving aluminum nitrate in distilled water; yttrium oxide is dissolved in 67 % HNO_3 by stirring the mixture for 3 h at about 80 ºC in a beaker covered with a glass slide. The mixture of the salt solutions (stoichiometric molarity of the Y^{3+} and Al^{3+} is maintained at 3:5 and the Y^{3+} concentration of the mixture is 2 mol L^{-1}) is put in the storage cup of a high-power ultrasonic reactor which was manufactured by Shen Zhen Xin Nuo Ke ultrasonic equipment Co. Ltd. The maximum ultrasonic power is 2 KW and the cross-sectional area of the probe is 5 mm^2. As Fig. 1 shows, the components of the apparatus are listed as follows: (1) three reactant liquid-storage cups; (2) reactor; (3) ultrasonic probe; (4) temperature detector; (the temperature of reaction system may rise greatly in the process of strong pulse ultrasonic); (5) ultrasonic controller; It can control the pulse width from 0.001-100 s and regulate the pulse duty factor and strength. Put 1.6 mol L^{-1} solution of ammonium hydrogen carbonate (AHC) into a 250 mL glass beaker and merge the ultrasonic probe 1 centimeter beneath the surface of AHC solution. Set the pulse duty factor to 1, power to 2 KW, pulse width to 0.5 s and start the high power ultrasonic apparatus. The dripping speed of the mother salt solution is so regulated that they must synchronize with time sequencing of the ultrasonic pulse to ensure this co-precipitation takes place in the working period of the ultrasound by revolving the glass knob. Another 10 min continuous ultrasound is needed after the titration of mother salt solution is over. The resulting suspension, after aging 24 h, is filtered using a suction filter, washed several times with distilled water and absolute alcohol to remove the soluble impurities. Dried at 1000 ºC for 8 h, the resultant YAG precursors are obtained, which are later calcinated at 400, 700, 800, 900, 1000 and 1100 ºC for 2 h, respectively.

X-ray powder diffraction patterns were recorded at room temperature on a Bruker diffractometer model D8 advance using Cu K_α radiation at scanning step 0.02º and scanning rate 0.5º/min. Tube power is 35KvX45 mA. Topas 3.0 was used to separate $K_{\alpha 2}$ from $K_{\alpha 1}$. The whole X-ray pattern is fitted by GSAS (general structure analysis system)[10], a free software created by Larson and Dreele of American Los Alamos National Laboratory for the Rietveld refinement of structural models to both X-ray and neutron diffraction data. The grain size and lattice strain are calculated according to eqns. 1 and 2.

$$P = \frac{18000K\lambda}{\pi x} \quad (1) \qquad S = \frac{\pi}{18000}(Y - Y_i) \times 100\,\% \quad (2)$$

where K is the Scherrer constant, X and Y are the peak profile refinement parameter LX and LY, respectively, Y_i is the profile parameter of reference sample without micro-strain. The units are Å. Thermal decomposition analysis was performed on a Seiko thermal analyzer model 6300 from temperature region 25-1000 ºC in air. The heating rate is 10 K min^{-1}. Infra-red spectrum is recorded on a shimadzu FT-IR model 8900 (resolution 4 cm^{-1}) using the standard KBr technique. SEM measurements are operated on Hitachi S-4700 with accelerating voltage 15KV and emission current 9500 nA (resolution 1.5 nm). Energy dispersive spectroscopy is performed on the same equipment with 30 KV accelerating voltage and 30° take-off angle.

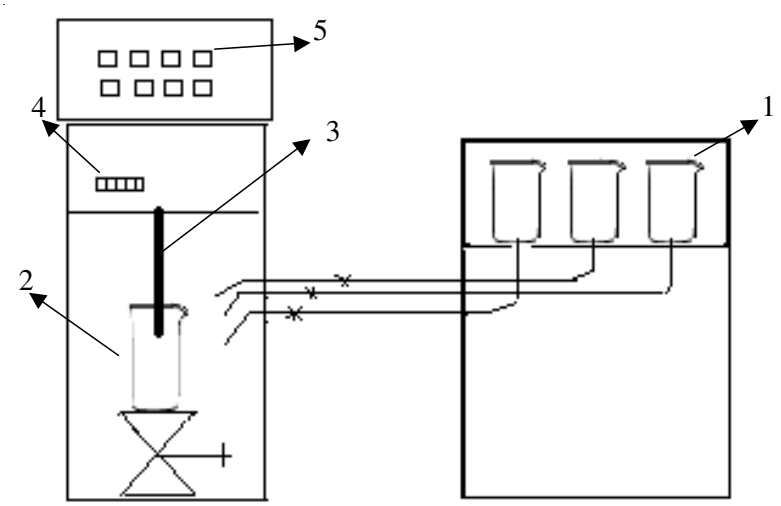

Fig. 1. Sketch of ultra-high power pulse ultrasonic reactor. (1) liquid storage cup; (2) reactor; (3) ultrasonic probe; (4) temperature detector; (5) ultrasonic controller

RESULTS AND DISCUSSION

XRD analysis of precipitation precursor calcinated at various temperatures: Fig. 2 shows the X-ray diffraction patterns for precursor powders calcinated at 400, 700, 800, 900, 1000 and 1100 ºC for 2 h, respectively. The co-precipitated powders are found to be amorphous until about 800 ºC, where small diffraction peaks typical of yttrium aluminum garnet $Y_3Al_5O_{12}$ (YAG) (JCPDS card no. 33-40) appear and this indicates the gradual crystallization of precursors. From 900 ºC, further calcinating at higher temperatures leads to the enhancement in the YAG diffraction peak intensity and reduces the full-width at the half-maximum due to the improvement of crystallization and crystal growth. In present studies, the temperature where crystallization starts is even lower than that in previously reported literature[11]. Moreover, YAG appears to crystallize directly from the amorphous precursor without the formation of any intermediate phase like YAM and YAP, indicating higher cation homogeneity of the precursor.

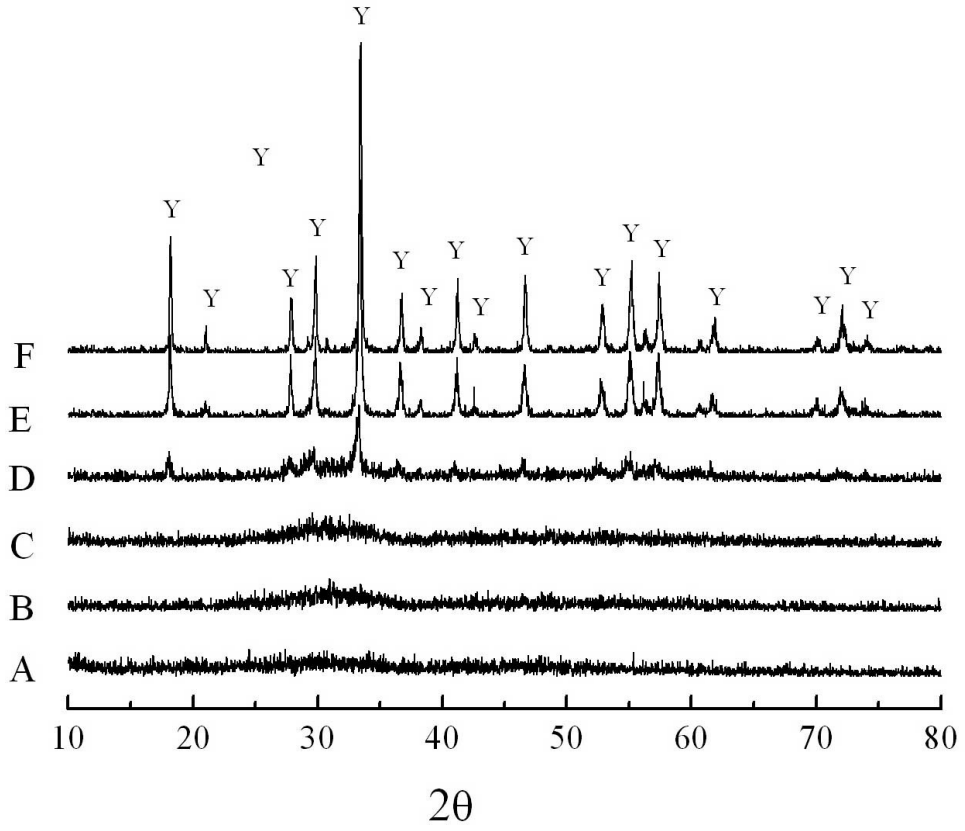

Fig. 2. XRD patterns of yttrium aluminum garnet (YAG) precursor (A) calcinated for 2 h at (B) 400, (C) 700, (D) 800, (E) 900 and (F) 1000 ºC, respectively

Rietveld refinement software GSAS (general structure analysis system) is used here. Parameters including cell parameters, atomic coordination, UISO, background, scaling, profile parameters GU, GV, GW, LX, LY, S/L, H/L, trans, shft, preferential orientation are refined. Appropriate refinement sequence is selected and after some cycles of refinement, the convergence is achieved. The refined results are listed in Table-1 and the ultimate Rietveld refinement results of YAG precursor calcinated at 1000 ºC for 2 h is shown in Fig. 3. The calculated pattern matches the observed pattern well.

TABLE-1
RESULTS OF RIETVELD REFINEMENT BY GSAS

Temp. (ºC)	Cell parameters (Å)			D (nm)	e (%)
	a	b	c		
1000	12.040	12.040	12.040	65	0.3
1100	12.012	12.012	12.012	92	0.2

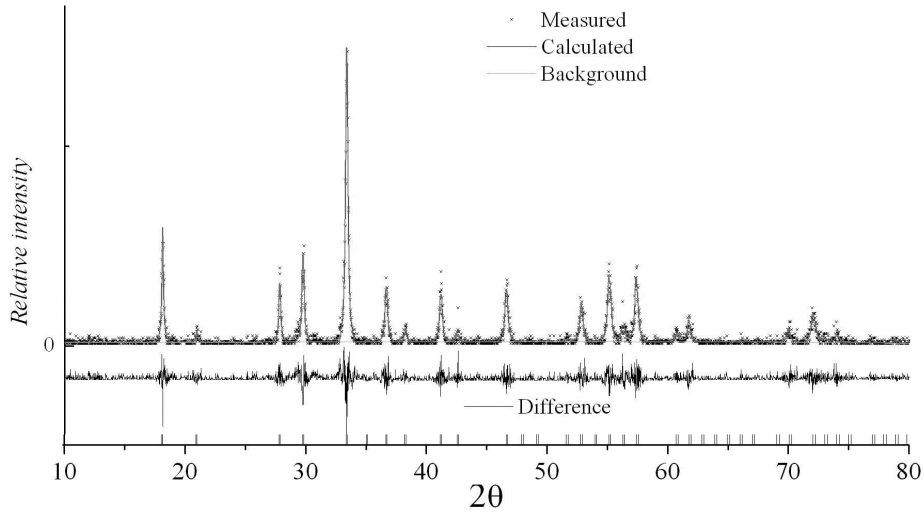

Fig. 3. Rietveld whole pattern fitting of the yttrium aluminum garnet (YAG) precursor calcinated at 1100 ºC.

Relatively large lattice distortion and expansion can usually be observed in the case of nano-particles for the repulsive dipole-dipole interaction between neighbouring grains, which is reported previously[12]. Especially under the experimental conditions here, large quantities of nuclei nucleate spontaneously, leading to the smaller grain size, incomplete crystal lattice and large lattice strain. Therefore, polycrystalline YAG exhibits large cell parameters and lattice expansion at the early stage of crystallization (Table-1). They gradually diminish and come close to the values of perfect YAG crystals with the release of lattice strain from 0.3 % in case of calcinating temperature 1000 ºC to 0.2 % at 1100 ºC, indicating improvement of lattice integrity when calcinating temperature further increases. In this process, crystal grows from 65-92 nm.

TG/DTA measurement of precipitate precursors: The weight lost below 600 ºC accounts for 80 % of overall weight loss (Fig. 4), there into 25.2 % of weight loses between room temperature and 200 ºC. Two discrete endothermic peaks are observed on the corresponding DTA curves. The desorption of adsorbed water and part of the crystal water possibly explain the endothermic peak at 106.8 ºC and that at 183.5 ºC is owing to the partial condensation of hydroxyl groups in $Al(OH)_3$. Calculated mass loss 26.3 % (16.9 % adsorbed water plus 9.4 % of $Al(OH)_3$ dehydration) matches the observed value well. The next small endothermic peak at *ca*. 460 ºC is related to the decomposition of carbonate among region 400-600 ºC. According to the binding ability of OH^- and CO_3^{2-}, when ammonia hydrogen carbonate solution is introduced into the aluminum nitrate, both $NH_4Al{\cdot}(OH)_2CO_3$ and $Al(OH)_3$ can possibly exist. However, the possibility of the existence of $NH_4Al{\cdot}\ (OH)_2CO_3$ is believed to have been significantly reduced because $NH_4Al{\cdot}(OH)_2CO_3$ strongly

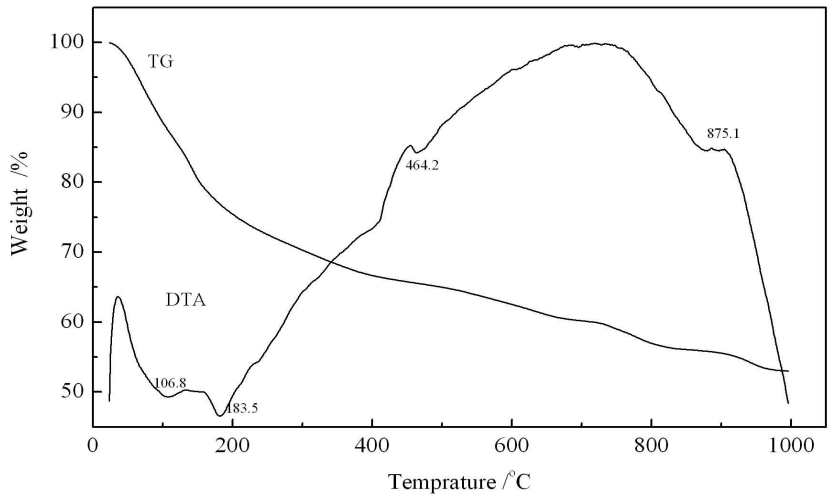

Fig. 4. TG/DTA curves of yttrium aluminum garnet (YAG) precursor

hydrolyzes influenced by the cavitation effect of high power ultrasonic, which are further substantiated by the strong hydroxyl absorbance on IR spectra of precursor. According to the work of Saito[13], the compositon of the resultant is supposed to be $Y_2(CO_3)_3$ when ammonium hydrogen carbonate is introduce into $Y(NO_3)_3$ solution. Therefore, the composition of precursor can be approximately expressed as $10[Al(OH)_3]\cdot 3[Y_2(CO_3)_3\cdot 7H_2O]$ with calculated overall weight loss 46.8 % as compared to the 46.7 % weight loss observed. Final exothermic peak at *ca.* 875.1 ºC is possibly pertaining to the crystallization of YAG from amorphous state. Amorphous precursors start crystallization near 800 ºC for the lagged exhibition of exothermic peak on DTA.

Infrared analysis of precipitation precursor calcinated at various temperatures: From the IR spectra of precipitation precursors (Fig. 5), strong absorption near 3500-3200 cm^{-1} is due to the stretching mode of H-O-H, with its bending mode near 1620 cm^{-1}. The intensity of -O-H absorption attenuates quickly, which disappear above calcinating temperature 400 ºC. Absorption bands at about 1533-1383 cm^{-1} correspond to the characteristic asymmetrical split stretching of carbonates, indicating the presence of CO_3^{2-}. The weak bands at 847-750 cm^{-1}, which are associated with the out-of-plane bending of CO_3^{2-}, further confirm the presence of the carbonates. With the elevating of treating temperatures, they attenuate gradually for the better thermal stability of carbonate. The absorption near 623 cm^{-1} is related to the stretching vibration of Al-O. Bands at about 795, 751, 687, 573 and 481 cm^{-1} characteristic of metal oxygen bond (M-O) vibration in the low wavenumber region 800-400 cm^{-1} gradually appear above 400 ºC, indicating the formation of YAG phase[14]. Interestingly, the absorption near 1510 cm^{-1} always exists even the calcinating temperature reaches as high as 1100 ºC and this is supposed to the frequency doubling of lattice vibration at about 751 cm^{-1}.

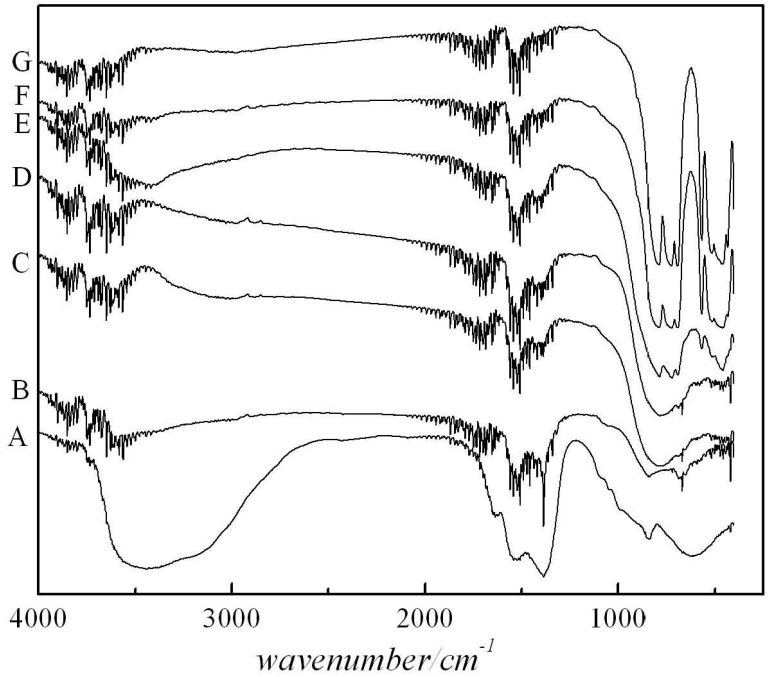

Fig. 5. IR spectra of yttrium aluminum garnet (YAG) precursor (A) calcinated for 2 h at (B) 400, (C) 700, (D) 800, (E) 900, (F) 1000 and (G) 1100 ºC, respectively

SEM/EDS measurement of precipitation calcinated at various temperatures: The ratios of Al:Y for YAG precursors calcinated for 2 h at 700, 800 and 1100 ºC, respectively, are listed in Table-2. The quantitative analysis for light elements is not accurate enough, only Al and Y elements are considered here. It is observed that the Al:Y ratio of YAG precursor is 2.14. With the increase of calcinating temperature, this ratio reaches maximum 2.38 at 400 ºC, then gradually decreases until it reaches minimum 1.45 at 1100 ºC, which is close to the Al:Y ratio in pure perfect YAG crystals $Y_3Al_5O_{12}$. According to the previous report that aluminum hydroxide usually precipitates earlier than yttrium carbonate and thus part of precipitated $Al(OH)_3$ is surface coated with $Y_2(CO_3)_3$ in that the solubility of aluminum hydroxide is much lower[15], A lower than usual Al:Y ratio seems reasonable. However, the contrary results are observed in present experiments. The extremely high temperature and pressure in region of acoustic cavitations, it is believed that the co-existence of high concentration of Al^{3+} and Y^{3+} ions with precipitants is really possible and the highly saturated ion species only precipitate spontaneously when this region is cooled rapidly with cooling rate as high as 10^{10} K/S. However, according to the procedure described in experimental section, $Al(NO_3)_3$ and $Y(NO_3)_3$ mixed solution is dripped in to the excess NH_4HCO_3 solution. Common ion effect enables the precipitation of $Y_2(CO_3)_3$ preceding $Al(OH)_3$ and the coating of $Al(OH)_3$ on the surface of pre-precipitated $Y_2(CO_3)_3$. This may explain the higher Al:Y ratio for the precursor.

With the increase of calcinating temperature, the loosely coated $Al(OH)_3$ can form dense coating framework *via* the dehydration and condensation. So, even higher Al:Y ratios are observed until the temperature reaches 800 ºC. When calcinating temperature further elevates, the diffusion of Y and Al elements becomes the dominant factors with decreased Al:Y ratios until finally they reach a steady value close to 1.67.

TABLE-2
Al:Y RATIOS OF YTTRIUM ALUMINUM GARNET $Y_3Al_5O_{12}$ (YAG) PRECURSOR CALCINATED AT DIFFERENT TEMPERATURES BY EDS

Mole ratio	precursor	800 ºC	900 ºC	1100 ºC	$Y_3Al_5O_{12}$
Al:Y	2.14	2.38	1.93	1.45	1.67

Fig. 6 shows the SEM photograph of the precursor (A) and calcinated at (B) 1100 ºC for 2 h. In case of precursor, 50-60 nm particles stack randomly. For YAG powders after calcination at 1100 ºC, irregular shaped structures most of which are flakes are observed. Those discrete flakes with 200-300 nm long and 60-70 nm wide are composed of 50-60 nm single crystals calculated according to X-ray diffraction. Those 60-70 nm single crystals can also be found randomly on the surface of the larger flakes according to the photograph presented. Although the grain sizes increase with increasing calcinating temperature, relatively good dispersity persists.

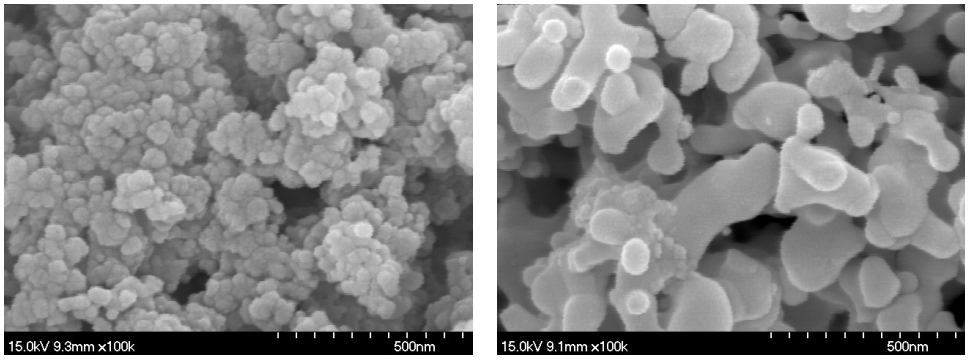

(A) (B)

Fig. 6. SEM photographs of yttrium aluminum garnet (YAG) precursor (A) and calcinated at (B) 1100 ºC for 2 h

Conclusion

Yttrium aluminum garnet ($Y_3Al_5O_{12}$, YAG) precursors are synthesized by ultra-high power ultrasonic (2 KW) assisted liquid phase co-precipitation with relatively high concentration reactants (2 mol L^{-1} Y^{3+}). Aluminum and yttrium constituents are evenly distributed. Yttrium aluminum garnet precursors begin to crystallize when calcinated for 2 h at relatively low temperature (800 ºC) without the appearance of any intermediate phase like YAP and YAM. Rietveld refinements show that poly-

crystalline YAG exhibits large cell parameters and lattice expansion at the early stage of crystallization. They gradually diminish and come close to the values of perfect YAG crystals with the improvement of lattice integrity and the release of lattice strain when the calcinating temperatures increase.

According to the results of thermal analysis, the composition of precursor can be approximately expressed as $10[Al(OH)_3]\cdot 3[Y_2(CO_3)_3\cdot 7H_2O]$ with calculated overall weight loss 46.8 % as opposed to the 46.7 % weight loss observed.

SEM/EDS characterization of YAG precursors calcinated at various temperatures indicates that the precipitation of Y^{3+} and Al^{3+} ions does not really happen spontaneously scrutinized at a smaller time interval though the whole process is normally called co-precipitation. $Y_2(CO_3)_3$ precipitates earlier than aluminum hydroxide and thus part of precipitated $Y_2(CO_3)_3$ is surface coated with aluminum hydroxide. With the increase of calcinating temperature, Al:Y ratios vary accordingly.

ACKNOWLEDGEMENTS

The authors gratefully acknowledge the support for this work from Zhejiang Natural Science Foundation (Grant No. Y407058), Ningbo Science & Technology Bureau Project (Grant No. 2006B100064, Grant No. 2008A610060) and K.C. Wong Magna Fund in Ningbo University.

REFERENCES

1. Y. Harada, T. Suzuki, K. Hirano, N. Nakagawa and Y. Waku, *J. Eur. Ceram. Soc*., **25**, 1275 (2005).
2. J. Lu, J. Song, M. Prabhu, C. Li, J. Xu, K. Ueda, H. Yagi, A. Kaminskii and T. Yanagitani, *Jpn. J. Appl. Phys*., **39**, 1048 (2000).
3. T.A. Parthasarathy, T. Mah and K. Keller, *Ceram. Eng. Sci*. **12**, 1767 (1991).
4. J. Alkebro, S. B. Colin, A. Mocellin and R. Warren, *J. Eur. Ceram. Soc.*, **20**, 2169 (2000).
5. Z.H. Sun, D.R. Yuan, H.Q. Li, X.L. Duan, H.Q. Sun, Z.M. Wang, X.C. Wei, H.Y. Xu, C. Luan, D. Xu and M.K. Lv, *J. Alloys Compd*., **379**, L1 (2004).
6. X. Li, H. Liu, J.Y. Wang, H.M. Cui and F. Han, *J. Am. Ceram. Soc*., **87**, 2288 (2004).
7. M.B. Kakade, S. Ramanathan and P.V. Ravindran, *J. Alloys Compd*., **350**, 123 (2003).
8. Z.H. Chen, Y. Yang, Z.G. Hu, J.T. Li and S.L. He, *J. Alloys Compd*., **433**, 328 (2007).
9. C. Burda, X.B. Chen, R. Narayanan and M.A. El-Sayed, *Chem. Rev.*, **10**, 1025 (2005).
10. C.A. Larson and B.V. Robert, GSAS Manual, Los Alamos National Laboratory Report LAUR pp. 86-748 (2004).
11. J.G. Li, T. Ikegami, J.H. Lee, T. Mori and Y. Yajima, *J. Eur. Ceram. Soc.*, **20**, 2395 (2000).
12. M.N. Rahaman, Ceramic Processing and Sintering, New York: Marcel Dekker, pp. 201-205 (1995).
13. N. Saiton, S. Matsudas and T. Ikegamit, *J. Am. Ceram. Soc*., **81**, 2023 (1998).
14. W.S. Peng and G.K. Liu, Infra-red Spectra for Inorganic Minerals, Peking: Science Press, pp. 306-308 (1982).
15. H.Z. Wang and L. Gao, *J. Inorg. Mater*., **15**, 630 (2001).

(*Received*: 12 March 2009; *Accepted*: 14 December 2009) AJC-8176